

Another Look at High-Alpha Support Interference in Rotary Tests

L. E. Ericsson*

Lockheed Missiles & Space Company, Inc., Sunnyvale, California 94089

Aerodynamic interference effects are generated by the model support structure, which in the case of rotary rigs can be very bulky. Further complicating the task of dynamic simulation in subscale tests is the fact that the measured effect of Reynolds number may be contaminated by support interference effects. In the present paper, recent experimental results, complementing those used in an earlier study, are examined, reconfirming and extending the conclusions reached at that time. An approach is formulated that can lead to a satisfactory solution of the problem of how to determine the coupled effects of support interference and subscale Reynolds number.

Nomenclature

<i>b</i>	= wing span
<i>c</i>	= reference length, mean aerodynamic chord or <i>d</i> for body alone
<i>d</i>	= maximum body diameter
<i>L</i>	= lift, coefficient $C_L = L/\bar{q}_\infty S$
<i>l</i>	= rolling moment, coefficient $C_l = l/\bar{q}_\infty Sb$
<i>M</i>	= freestream Mach Number
<i>m</i>	= pitching moment, coefficient $C_m = m/\bar{q}_\infty Sc$
<i>N</i>	= normal force, coefficient $C_N = N/\bar{q}_\infty S$
<i>n</i>	= yawing moment, coefficient $C_n = N/\bar{q}_\infty Sb$
<i>p</i>	= pressure, coefficient $C_p = (p - p_\infty)/\bar{q}_\infty$
<i>q</i>	= dynamic pressure, $\rho U^2/2$
<i>Re</i>	= Reynolds number, $U_\infty c/\nu_\infty$
<i>S</i>	= reference area, effective wing area or $\pi d^2/4$ for body alone
<i>U</i>	= wind-fixed axial velocity
<i>V</i>	= lateral velocity
<i>x</i>	= axial distance from body apex, positive aft
<i>Y</i>	= side force, coefficient $C_Y = Y/\bar{q}_\infty S$
α	= angle of attack
β	= angle of sideslip
Δ	= increment
ν	= kinetic viscosity
ρ	= density of air
ϕ	= coning angle, roll angle of rotary rig around its axis
φ	= body-fixed roll angle
Ω	= dimensionless coning rate, $\dot{\phi}b/2U_\infty$

Subscripts

<i>A</i>	= apex
<i>S</i>	= sting
∞	= freestream conditions

Differential Symbols

$\dot{\phi}$	= $\partial\phi/\partial t$: $C_{\dot{\phi}} = \partial C_\phi/\partial\beta$
--------------	--

Introduction

IN the case of static tests, the aerodynamic support interference problem has been studied extensively,¹⁻³ and guidelines have been established for how to select support geometry

Presented as Paper 90-0188 at the AIAA 28th Aerospace Sciences Meeting, Reno, NV, Jan. 8-11, 1990; received Feb. 2, 1990; revision received July 15, 1990; accepted for publication Aug. 3, 1990. Copyright © 1990 by L. E. Ericsson. Published by the American Institute of Aeronautics and Astronautics, Inc., with permission.

*Senior Consulting Engineer, 1111 Lockheed Way. Fellow AIAA.

and model size in order to ensure that the aerodynamic interference remains insignificant. In dynamic tests, however, it is often not possible to reduce the interference to the level of insignificance. For a forced oscillation test, for example, the support structure is much bulkier than in a static test, aggravating the problem of aerodynamic interference.^{4,5} The problem of aerodynamic interference increases both in severity and complexity when performing tests at high angles of attack, where body and wing vortices can interact with the support structure. The support becomes massive in the case of the rotary rig because of the high stiffness needed to avoid excessive deflections and vibrations in the presence of the large, unbalanced centrifugal forces generated by the coning motion.^{6,7}

Discussion

Because of its bulkiness, the rotary rig often causes a significant change of the flowfield in the test section, even in the absence of the model to be tested, as has been observed for the rotary rigs both at DFVLR⁸ and ONERA-IMFL⁹ (Fig. 1). By itself, a longitudinal dynamic pressure gradient can have a significant effect, not only on fin effectiveness, but more important, on boundary-layer transition and/or flow separation. By using a slight area contraction over the length of the test section, the blockage effect of the rotary rig could be compensated for, practically eliminating the longitudinal dynamic pressure gradient with its potentially large effect on the development of separated flow at high angles of attack⁹ (Fig. 1). A similar blockage effect may have contributed to the poor agreement of the C_m (α) measurements using a rotary rig with those obtained in static tests with less bulky support structures¹⁰ (Fig. 2). Also contributing to the difference between the experimental results was, in all likelihood, the interaction between the vortices from the aircraft model and the bulky rotary-rig support structure, a problem that will be discussed later. The balance sector accounts for approximately half of the support blockage effect on the flow in the empty test section. The effect of the upwash, generated by the rotating balance arm (at the location of a model to be tested), has, however, been found to be negligible.¹¹ It is important to eliminate the support blockage effect on the basic flowfield in the empty test section before considering the more difficult problem of the interference effect of the rotary rig on the flowfield generated by the model.¹²

Figure 3 shows the lateral static stability characteristics measured at $\alpha = 35$ deg using two different support systems.¹³ Both support systems can cause significant interference.⁴ However, only the support with a downstream balance sector is likely to cause early breakdown of vortices generated by a slender forebody at high angles of attack, or of the leading-edge

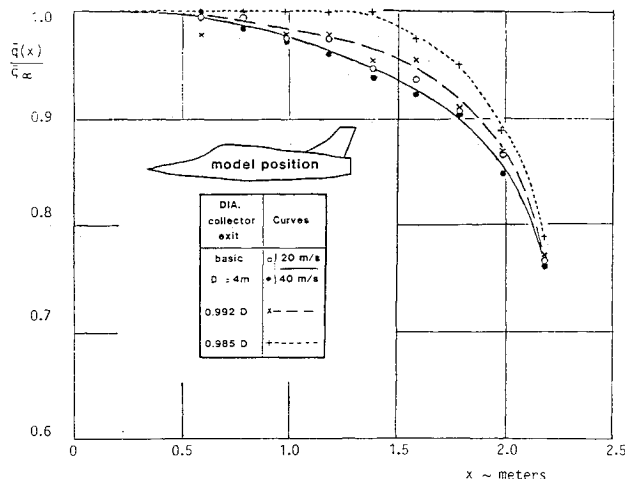


Fig. 1 Elimination of support-induced dynamic pressure gradient by control of test section exit diameter.⁹

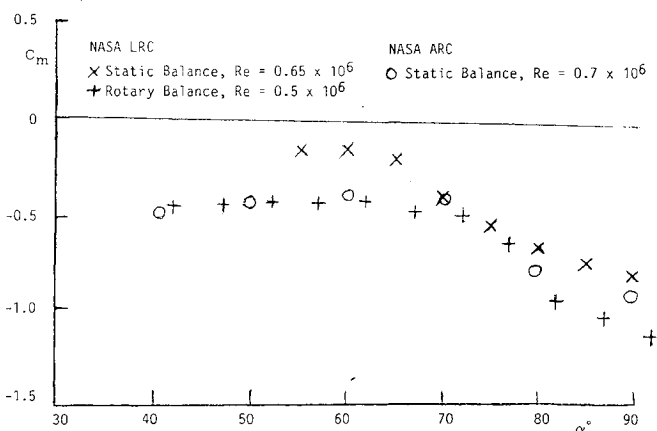


Fig. 2 Effect of model support on the pitching moment of an advanced aircraft model.¹⁰

vortices from a slender wing for a certain range of sideslip angles. This is the conclusion to be drawn from the repetition of Hummel's classic experiment¹³ (Fig. 3) using an arrow wing¹⁴ (Fig. 4).

Support Interference

The vortices generated by a slender nose¹⁵⁻¹⁷ can interact with a downstream support, especially at very high angles of attack when the vortices become asymmetric. In this case, one vortex is left close to the fuselage¹⁸ (Fig. 5). One realizes that the support interference on an asymmetric vortex pair of the type shown in Fig. 5 can be large, as the active (lower) vortex moves close to the symmetry plane.^{17,19} Figure 6 shows the support interference to be very different for the inclinations $\alpha_s = 45$ and 70 deg of the top-mounted sting, causing interference effects of opposite sign in the region of steady asymmetric vortex shedding.²⁰ Although the region of steady asymmetric vortex shedding can be extended beyond the usual limit, $\alpha \approx 60$ deg, as has been discussed,²¹ at $\alpha \approx 90$ deg the vortex shedding should be of the unsteady type, giving a time average value $C_n = 0$. The nonzero values in Fig. 6 are likely to have been caused by splitter-plate-like interference, such as that found by Dietz and Alstatt.²²

In the case of a coning test, the angle α_s affects the C_n characteristics at all angles where asymmetric vortex shedding occurs.²⁰ The results at $\alpha = 70$ deg (Fig. 7) are apparently of the critical type.²³ Thus, the asymmetric vortex geometry is affected strongly by moving-wall effects,^{23,24} causing the vortex asymmetry to flip between its two extreme positions, with associated reversals of the yawing moment (Fig. 7).

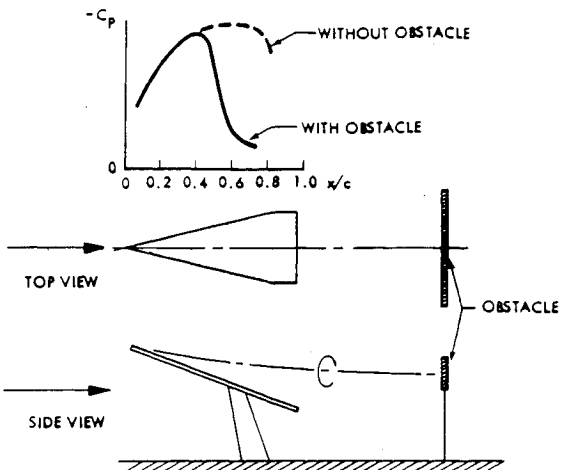


Fig. 3 Vortex burst on a 75-deg delta wing caused by downstream obstacle.¹³

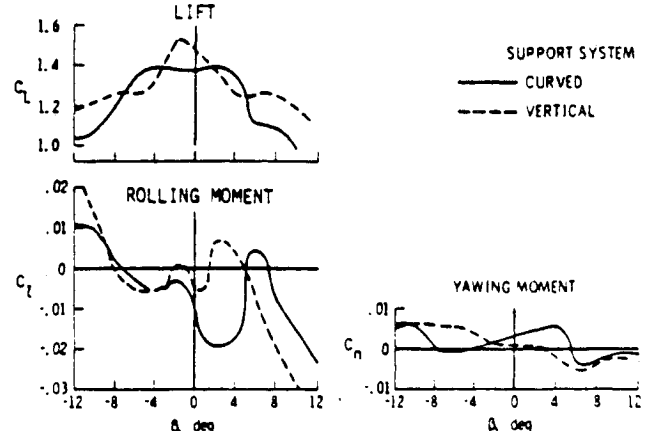
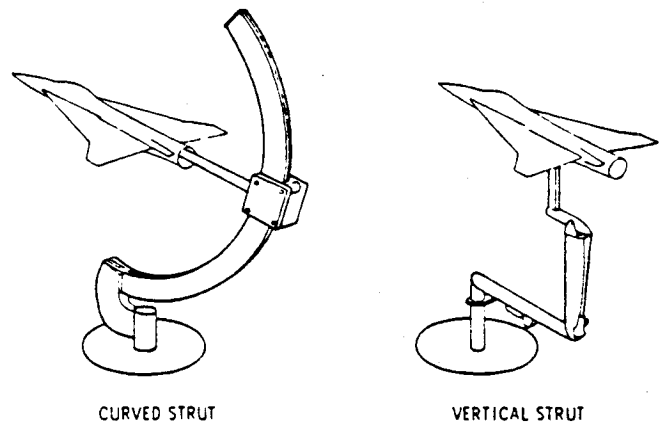


Fig. 4 Effect of model support on the lateral characteristics of an arrow wing aircraft model.¹⁴

Recent tests of the High Incidence Research Model HIRM 2 model²⁵ (Fig. 8) show that, when using a top-mounted dummy sting in addition to the aft sting support, the dummy sting added significantly to the support interference at $\alpha = 40$ and 60 deg, whereas the effect at $\alpha = 50$ deg was insignificant. Furthermore, at $\alpha = 40$ deg (Fig. 8a), the rolling moment is affected substantially, whereas at $\alpha = 60$ deg (Fig. 8c), only the yawing moment shows any appreciable influence.

Similar tests have been performed at AerMacchi²⁶ (Fig. 9). At $\alpha = 45$ deg, the aircraft model should generate asymmetric forebody vortex shedding. The nose apex half angle is approximately 15 deg, suggesting that asymmetric vortex shedding started at $\alpha \approx 30$ deg.¹⁵⁻¹⁷ In this case, there was no apparent

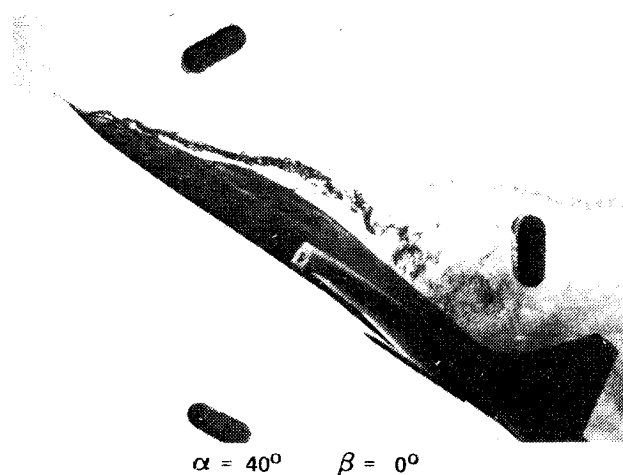


Fig. 5 Asymmetric vortex shedding from the slender nose of an advanced aircraft model.¹⁸

effect of changing between forward and aft sting supports. One obvious interpretation of these test results is that the support interference was so large for the rear sting arrangement, caused more by the balance arm than the rear strut, that placing the sting support forward of the fin had no significant effect. Judging by Hummel's test results¹³ (Fig. 4), the balance arm easily could have caused vortex burst to occur forward of the fin, in which case the forward sting would only have the effect of moving the vortex burst farther upstream. As the vortex-induced fin loads were already lost for the aft burst location, the forward sting would not have a very significant effect on the aerodynamic characteristics. In contrast, when the sideslip was increased from $\beta=0$ (Fig. 9a) to $\beta=10$ deg (Fig. 9b), the difference between interference from the two support systems became more significant. Of particular interest is the change of interference effects occurring at $\Omega \approx 0.1$. What can be the reason for this?

In Ref. 12, it is described how the various support interference results obtained by Malcolm in his coning experiments²⁰ can be explained when considering how the support amplifies

the coning-induced bias of the forebody vortices. Another way of inducing such a bias is by setting the model at an angle of sideslip. Even without the occurrence of vortex burst, the support will amplify the displacement of the vortex induced by sideslip and/or coning.

Tobak et al.²⁷ found in their coning test of an ogive cylinder that the symmetric vortex geometry was tilted at an angle $\Delta\varphi_A$ along the full length of the body, where $\Delta\varphi_A$ is determined by the coning-induced lateral velocity at the apex:

$$\Delta\varphi_A = \tan^{-1}(V_A/U_\infty) \quad (1a)$$

$$\frac{V_A}{U_\infty} = \frac{x_{c.g.} \sin\alpha}{b} \frac{\dot{\phi}b}{U_\infty} \quad (1b)$$

Borrowing the coning sketch from Ref. 28 (see Fig. 10), one can see that the vortex will be displaced in the same sense for $\dot{\phi} > 0$ as for $\beta > 0$. The tilt angle corresponding to $\Delta\varphi_A$ in Eqs. (1) is

$$\Delta\varphi(\beta) = \tan^{-1}(\sin\beta \cot\alpha) \quad (2)$$

For $x_{c.g.}/b \approx 1$ and $\alpha = 45$ deg, Eqs. (1) give $\Delta\varphi_A = \Omega\sqrt{2}$, which for $\Omega = 0.1$ gives $\Delta\varphi_A \approx 8$ deg. For $\alpha = 45$ deg, Eq. (2) gives $\Delta\varphi(\beta) = \tan^{-1}(\sin\beta) \approx \beta$. That is, when considering the fact that the tilting of the vortex system will be amplified by moving-wall effects,^{23,24} one can expect $\Delta\varphi_A$ and $\Delta\varphi(\beta)$ to be of roughly the same magnitude for $\Omega = 0.1$ and $\beta = 10$ deg, respectively. Following the analysis in Ref. 12, one can interpret the data for $\beta = 10$ deg in Fig. 9b to show that, when $\Delta\varphi_A$ is added to $\Delta\varphi(\beta)$ at $\beta = 10$ deg, the active forebody vortex misses the rear strut.

Thus, using the rear sting makes it possible to measure the effect of the interaction between the (lower) forebody vortex and the tail at $\beta = 10$ deg and $\Omega > 0.1$, whereas the dorsal sting, because of its closeness to the vortex-generating forebody, bursts the vortex and makes such a measurement impossible. It is, in fact, suggested in Ref. 11 that the dorsal sting made it impossible to measure the true nonlinear coning characteristics. It needs to be emphasized, however, that the important observation to be made is not that the true nonlinear coning characteristics could be measured at $\beta > 10$ deg and $\Omega > 0.1$, if

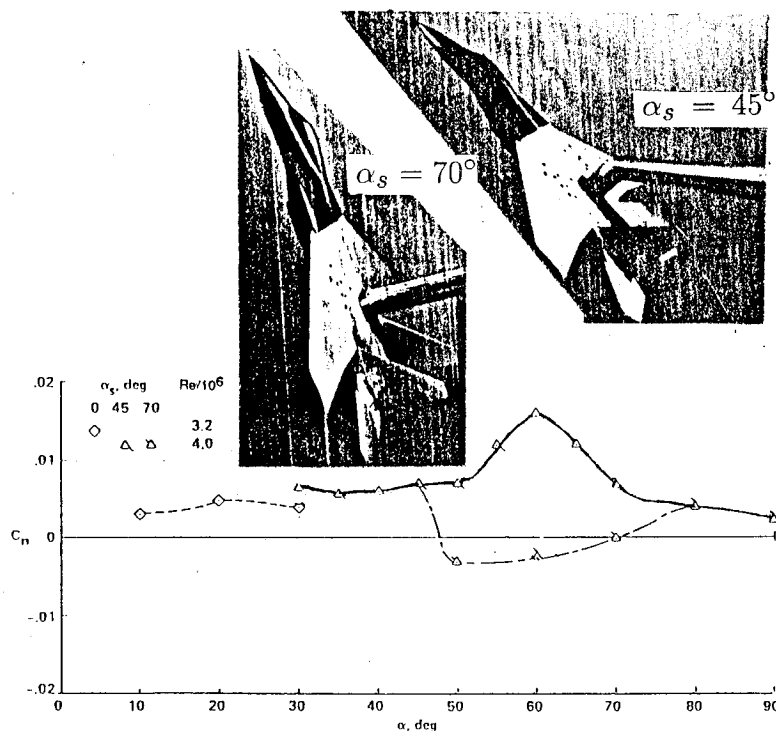


Fig. 6 Effect of support inclination α_s and Reynolds number at $\beta=0$ on an advanced aircraft model with nose boom.

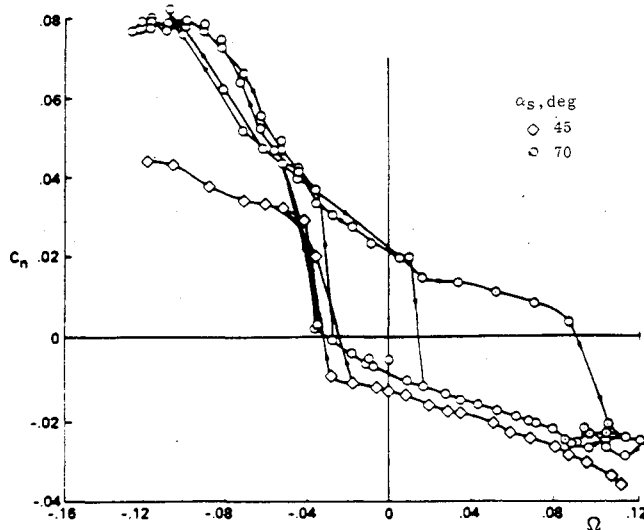


Fig. 7 Effect of support inclination α_s on an advanced aircraft model with nose boom at $\beta=0$ and $Re=1.5 \times 10^6$ (Ref. 10).

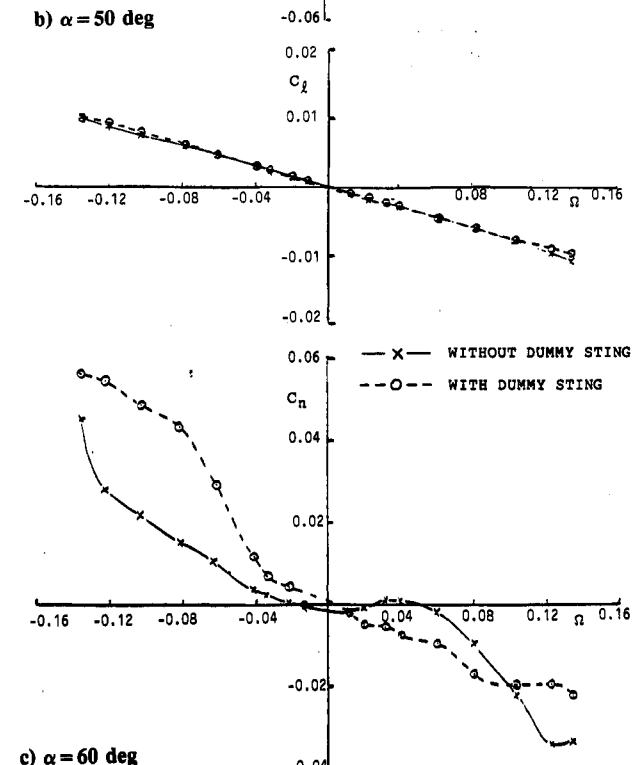
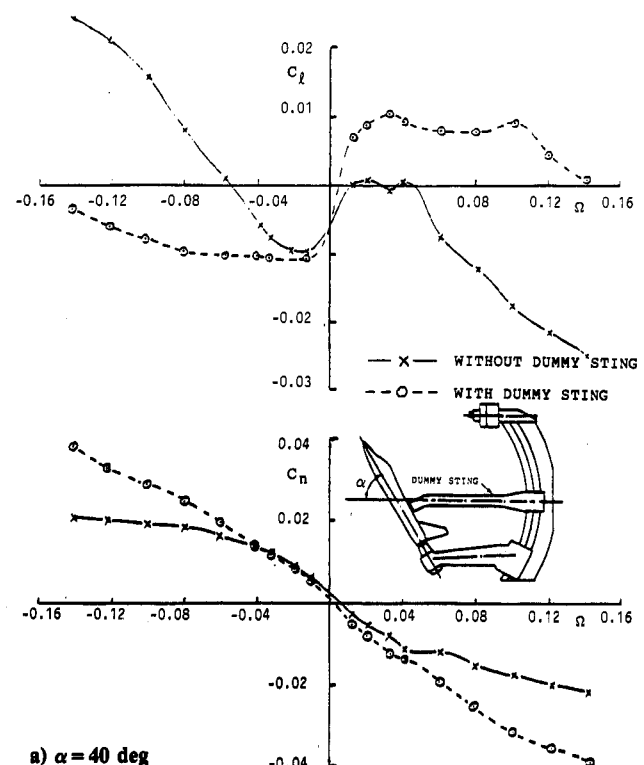
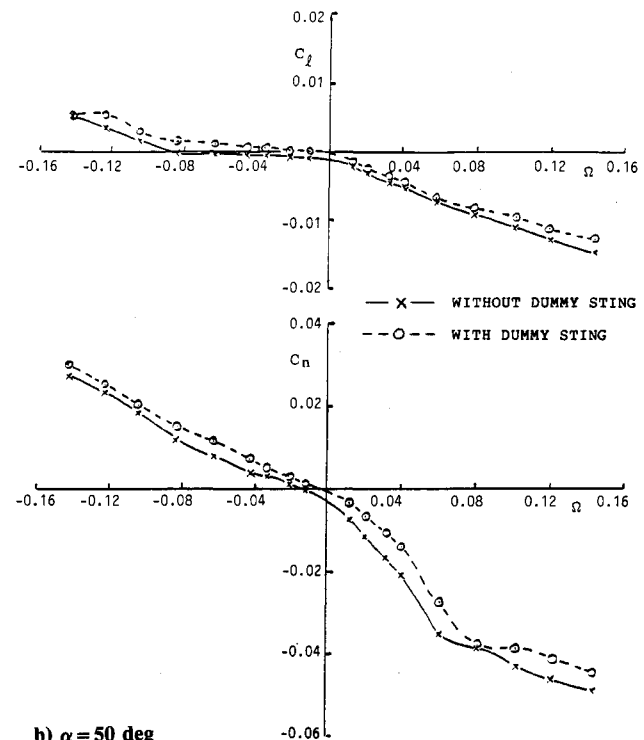


Fig. 8 Effect of dummy sting on coning characteristics $C_l(\Omega)$ and $C_n(\Omega)$ of the HIRM 2 Model at $M_\infty = 0.2$ and $Re = 0.9 \times 10^6$ (Ref. 25).

the rear sting support was used, but rather that both supports prevented the measurement of the true nonlinear coning characteristics at $\beta < 10$ deg and/or $\Omega < 0.1$. It is discussed in Ref. 12 how coning tests on a model of the F-15 aircraft,²⁰ performed for various sideslip angles, gave results for the combined effects of β and Ω that are similar to the results discussed here.

Support interference results, such as those shown in Figs. 2, 3, 8, and 9, are easy to misinterpret. Without additional experiments and careful analysis, the results tell next to nothing about the total support interference of either one of the two support systems used. They only show the difference

between the interference effects caused by the two supports. In the case of the very different support systems in Fig. 3, it can be shown that both supports produce significant interference.⁴ It is more obvious for the cases illustrated in Figs. 8 and 9 that the interference from the rear support and, in particular, the rotor arm is large to start with. Consequently, it should not be surprising that the addition of, or change to, an upstream sting support has little effect. It is more unusual that a significant effect sometimes is observed, although only for certain α - β - Ω combinations.

Whereas sideslip can eliminate the support interference on forebody vortices in a rotary test, it can introduce it for the

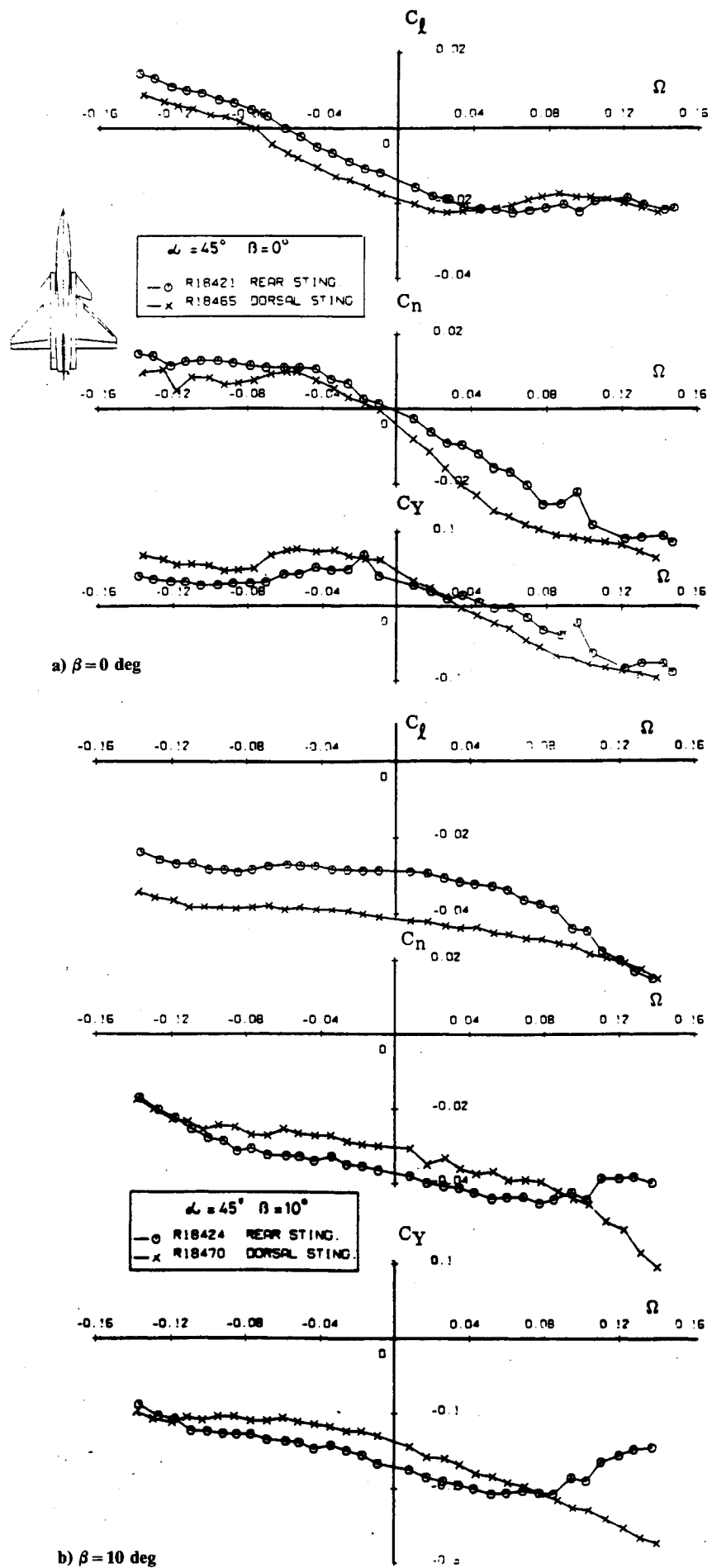


Fig. 9 Effect of model support change on the coning characteristics of a delta canard research configuration.²⁶

leading-edge vortices from highly swept wings, as the static test results in Fig. 11 illustrate. At $\alpha > 12$ deg, when the vortex-induced aerodynamic loads are becoming significant, the agreement between prediction²⁹ and experiment³⁰ starts to deteriorate because support interference on the upwind leading-edge vortex occurs at $\beta > 5$ deg (Fig. 12).

Coping with Support Interference

The test results in Figs. 8, 9, and 11 demonstrate that the support interference in high-alpha tests can be of significant magnitude. As in the case of tests at low-to-moderate angles of attack,^{4,5} one has to learn how to cope with this often unavoidable problem.^{31,32} As has been amply illustrated, the rotary apparatuses in use today are all likely to produce significant support interference over much of the testing envelope. In order to cope with this problem, the following steps should be taken: 1) identify the flow mechanism(s) through which the support interference acts, 2) design the support such that interference effects are minimized, and 3) if possible, derive the means through which the experimental results can be corrected for support interference. It appears that use of the orbital-platform concept,³³ which can provide close to interference-free test results, would be of great help in developing correction techniques.

In regard to step 1, aside from the blockage effect discussed earlier (Fig. 1), the main flow interaction causing high-alpha support interference is due to the obstruction presented by the

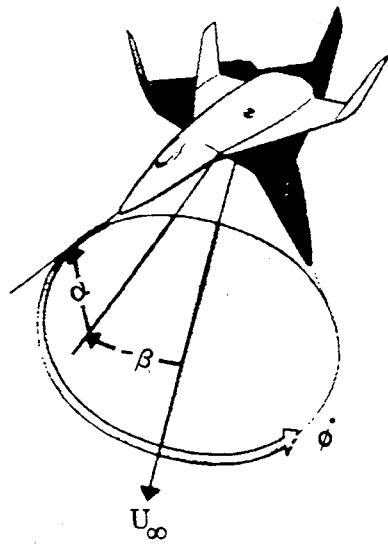


Fig. 10 Definition of variables for coning motions.²⁸

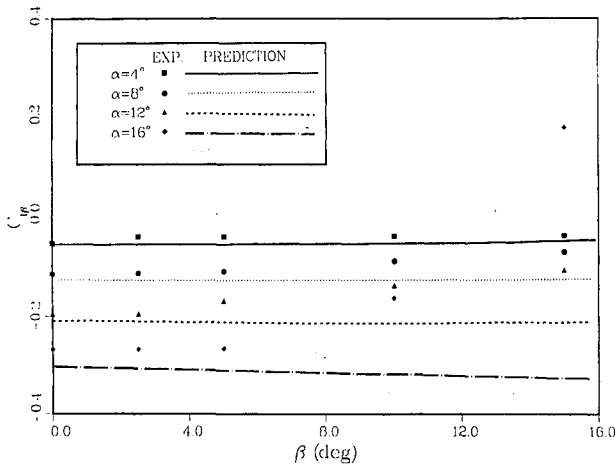


Fig. 11 Lateral stability characteristics of a 76-deg sharp-edged delta wing.²⁹

support to the vortical flowfield from a slender forebody and/or low aspect ratio lifting surfaces, as was illustrated by the examples in Figs. 3, 6, 8, 9, and 11. This support interference is strongly dependent upon the test section size and associated wall interference,³⁴ as was recently demonstrated²⁵ (Fig. 13).

In regard to step 2, some guidelines can be drawn from existing experimental results. As discussed earlier, top-

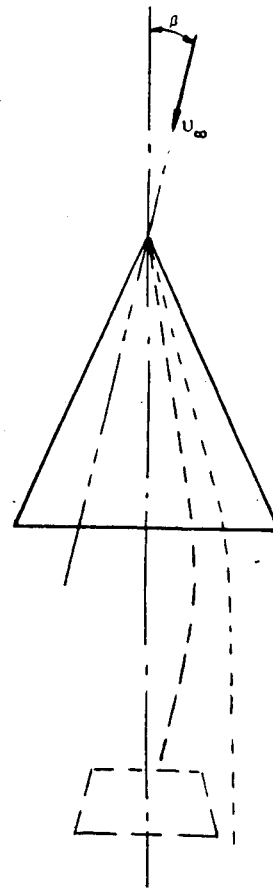


Fig. 12 Effect of sideslip on the support interference on the leading-edge vortex from a slender delta wing.

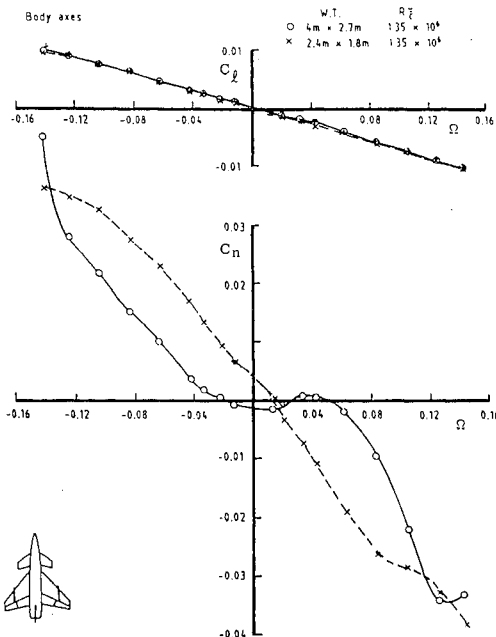


Fig. 13 Comparison of results from two wind tunnels of HIRM 2 coning characteristics.²⁵

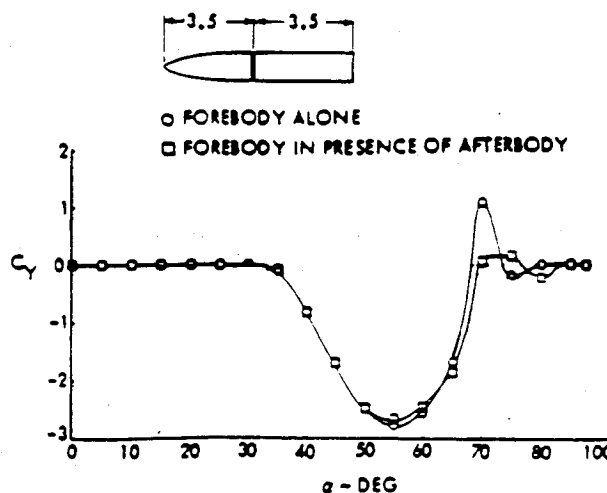


Fig. 14 Effect of cylindrical afterbody on the measured side force of a pointed ogive.³⁵

mounted supports should be avoided when steady asymmetric vortical flow exists. The results³⁵ in Fig. 14 demonstrate that an aft sting support by itself will not affect the vortical flowfield generated by a slender forebody. The problem is presented by the downstream balance arm and strut, to which the sting is connected, as it often can present enough of a flow obstruction to cause vortex burst.

In regard to step 3, correction for support interference will only be possible after systematic tests have been performed to provide the information needed for a meaningful analysis. It is shown in Ref. 5 how, by performing tests with a deflected sting, one could obtain static test data from which the support interference effect on the dynamic stability derivative in pitch could be determined. This low-alpha support interference is highly nonlinear, diminishing as the angle of attack is increased from $\alpha = 0$. At $\alpha > 10$ deg, it is practically nonexistent. As the angle of attack is increased further, however, at some point the interference from a downstream support on forebody and/or swept wing vortices starts to have a significant influence on the measured aerodynamic characteristics. Although the support geometry is more complex in the case of coning experiments than for one-degree-of-freedom oscillations in pitch or yaw, the fluid mechanics of support interference is simplified considerably. The coning motion is steady in nature, obviating the need to determine the time lag associated with the convection of the interference from the downstream support to the upstream model. (This is true only when the wall interference, discussed in Ref. 34, is negligible.) Thus, one only has to determine the static equivalent of the coning-induced displacement of the vortical wake or, at very high angles of attack, of the free vortices generated by a slender forebody and/or low aspect ratio lifting surfaces.

Aside from the usual problem of extrapolation from subscale test results to full-scale conditions,^{36,37} in the case of high-alpha tests one has to consider how the Reynolds number affects the vortex shedding from a slender body and, thereby, the associated support interference. A very important consideration in this regard is the large differences in moving-wall effects occurring when going from subcritical (laminar) through critical to supercritical (turbulent) flow conditions.²⁴ Thus, the support interference has to be investigated for the full range of flow conditions, from subscale to full-scale Reynolds numbers, before confident extrapolation from subscale rotary balance data to full-scale flight can be possible.

Conclusions

A review of recent experimental results has confirmed that measurements of dynamic characteristics obtained at high angles of attack, using equipment such as rotary balances, will

almost always be affected to a significant degree of support interference. It appears, however, that a concentrated effort by the high-alpha technical community could lead to the development of methods that could provide satisfactory correction for support interference effects.

References

- Perkins, E. W., "Experimental Investigations of the Effects of Support Interference on the Drag of Bodies of Revolution at a Mach Number of 1.5," NACA TN-2292, Feb. 1971.
- Whitfield, J. P., "Support Interference at Supersonic Flow," AGARD Rept. 300, March 1959.
- Kavanau, L. L., "Base Pressure Studies in Rarefied Supersonic Flow," *Journal of Aerospace Sciences*, Vol. 23, March 1956, pp. 193-207.
- Ericsson, L. E., and Reding, J. P., "Review of Support Interference in Dynamic Tests," *AIAA Journal*, Vol. 21, No. 12, 1983, pp. 1652-1666.
- Reding, J. P., and Ericsson, L. E., "Dynamic Support Interference," *Journal of Spacecraft and Rockets*, Vol. 9, No. 6, 1972, pp. 547-553.
- Orlik-Rückemann, K. J., "Techniques for Dynamic Stability Testing in Wind Tunnels," AGARD-CP-235, Nov. 1978.
- Ericsson, L. E., "A Summary of AGARD FDP Meeting on Dynamic Stability Parameters," AGARD-CP-260, May 1979.
- "Entwicklung und Erprobung einer Roll- und Trudelderivativ-Waage für die 3m-Niedergeschwindigkeitswindkanäle der Bundesrepublik Deutschland," Rept. EMFT-FB-W81-022, 1981.
- Verbrugge, R. A., "Balance Rotative de l'I.M.F.L. et Techniques Expérimentales Associées," Sept. 1979.
- Chambers, J. R., private communication, Sept. 1988.
- Visintini, L., "Short Summary of Information about Interference Effects due to the Rotary Balance Rig," AerMacchi, Varese, Italy, Memo PRA/0-05/86, May 1986.
- Ericsson, L. E., and Reding, J. P., "Dynamic Support Interference in High-Alpha Testing," *Journal of Aircraft*, Vol. 23, No. 12, 1986, pp. 889-896.
- Hummel, D., "Untersuchungen über das Aufplatzen der Wirbel an schlanken Delta Flügeln," *Zeitschrift für Flugwissenschaften*, Vol. 5, No. 3, 1965, pp. 158-168.
- Johnson, J. L., Jr., Grafton, S. B., and Yip, L. P., "Exploratory Investigation of Vortex Bursting on the High-Angle-of-Attack Lateral Directional Stability Characteristics of Highly Swept Wings," AIAA Paper 80-0463, March 1980.
- Ericsson, L. E., and Reding, J. P., "Review of Vortex-Induced Asymmetric Loads—Part I," *Zeitschrift für Flugwissenschaften und Weltraumforschung*, Vol. 5, No. 3, 1981, pp. 162-174.
- Ericsson, L. E., and Reding, J. P., "Review of Vortex-Induced Asymmetric Loads—Part II," *Zeitschrift für Flugwissenschaften und Weltraumforschung*, Vol. 5, No. 6, 1981, pp. 349-366.
- Ericsson, L. E., and Reding, J. P., "Asymmetric Vortex Shedding from Bodies of Revolution," *Tactical Missile Aerodynamics*, Vol. 104, Progress in Astronautics and Aeronautics, edited by M. J. Hemsch and J. N. Nielsen, AIAA, New York, 1986, pp. 243-296.
- Skow, A. M., Moore, W. A., and Lorincz, D. J., "Forebody Vortex Blowing—A Novel Control Concept to Enhance Departure/Spin Recovery Characteristics of Fighter and Trainer Aircraft," AGARD-CP-262, Sept. 1979.
- Wardlaw, A. B. J., and Yanta, W. J., "Multistable Vortex Patterns of Slender Circular Bodies at High Incidence," *AIAA Journal*, Vol. 20, No. 4, 1982, pp. 509-515.
- Malcolm, G. N., "Rotary-Balance Experiments on a Modern Fighter Aircraft Configuration at High Reynolds Numbers," AIAA Paper 85-1829, Aug. 1985.
- Ericsson, L. E., and Reding, J. P., "Alleviation of Vortex-Induced Asymmetric Loads," *Journal of Spacecraft and Rockets*, Vol. 17, No. 6, 1980, pp. 548-553.
- Dietz, W. E., and Alstatt, M. C., "Experimental Investigation of Support Interference on an Ogive-Cylinder at High Incidence," *Journal of Spacecraft and Rockets*, Vol. 16, No. 1, 1979, pp. 67, 68.
- Ericsson, L. E., and Reding, J. P., "Dynamics of Forebody Flow Separation and Associated Vortices," *Journal of Aircraft*, Vol. 22, No. 4, 1985, pp. 329-335.
- Ericsson, L. E., "Moving Wall Effects in Unsteady Flow," *Journal of Aircraft*, Vol. 25, No. 11, 1988, pp. 977-990.
- O'Leary, C. O., and Weir, B., "Effects of Reynolds Number, Mach Number and Sting Geometry on Rotary Balance Measurements," *Proceedings of the 17th Congress of the International Council*

cil of the Aeronautical Sciences, Vol. 2, AIAA, Washington, DC, Sept. 1990, pp. 1485-1495.

²⁶Visintini, L., private communication, April 1988.

²⁷Tobak, M., Schiff, L. B., and Peterson, V. L., "Aerodynamics of Bodies of Revolution in Coning Motion," *AIAA Journal*, Vol. 7, No. 1, 1969, pp. 95-99.

²⁸Jermey, C., and Schiff, L. B., "Wind Tunnel Investigation of the Aerodynamic Characteristics of the Standard Dynamics Model in Coning Motion at Mach 0.6," AIAA Paper 85-1828, Aug. 1985.

²⁹Ericsson, L. E., and King, H. H. C., "Rapid Prediction of Slender-Wing-Aircraft Stability Characteristics," AIAA Paper 90-0301, Jan. 1990.

³⁰Peckham, D. H., "Low-Speed Wing-Tunnel Tests on a Series of Uncambered Slender Pointed Wings with Sharp Leading Edges," Aerodynamic Research Council, UK, R&M No. 3186, Dec. 1958.

³¹Ericsson, L. E., and Reding, J. P., "Practical Solutions to Simulation Difficulties in Subscale Wind Tunnel Tests," AGARD Fluid Dynamics Panel Symposium on Wind Tunnels and Testing Tech-

niques, Paper 16, Sept. 1983.

³²Ericsson, L. E., and Reding, J. P., "How to Cope with the Problem of Scaling and Support Interference in Dynamic Subscale Tests," AIAA Paper 84-0382, Jan. 1984.

³³Bevers, M. E., and Huang, X. Z., "The Orbital-Platform Concept for Nonplanar Dynamic Testing," National Academy of Engineering, Ottawa, Canada, NAE-AN-52, NRC No. 29133, May 1988.

³⁴Bevers, M. E., "Unsteady Wall Interference in Rotary Tests," AIAA Paper 89-0046, Jan. 1989.

³⁵Keener, E. R., Chapman, G. T., and Kruse, R. L., "Effects of Mach Number and Afterbody Length on Onset of Asymmetric Forces on Bodies at Zero Sideslip and High Angles of Attack," AIAA Paper 76-66, Jan. 1976.

³⁶Ericsson, L. E., and Reding, J. P., "Scaling Problems in Dynamic Tests of Aircraft-Like Configurations," AGARD-CP-227, Feb. 1978.

³⁷Ericsson, L. E., and Reding, J. P., "Reynolds Number Criticality in Dynamic Tests," AIAA Paper 78-166, Jan. 1978.

*Recommended Reading from the AIAA
Progress in Astronautics and Aeronautics Series . . .* 

Thermal Design of Aeroassisted Orbital Transfer Vehicles

H. F. Nelson, editor

Underscoring the importance of sound thermophysical knowledge in spacecraft design, this volume emphasizes effective use of numerical analysis and presents recent advances and current thinking about the design of aeroassisted orbital transfer vehicles (AOTVs). Its 22 chapters cover flow field analysis, trajectories (including impact of atmospheric uncertainties and viscous interaction effects), thermal protection, and surface effects such as temperature-dependent reaction rate expressions for oxygen recombination; surface-ship equations for low-Reynolds-number multicomponent air flow, rate chemistry in flight regimes, and noncatalytic surfaces for metallic heat shields.

TO ORDER: Write, Phone or FAX:

American Institute of Aeronautics and Astronautics,
c/o TASCO, 9 Jay Gould Ct., P.O. Box 753, Waldorf, MD 20604
Phone (301) 645-5643, Dept. 415 • FAX (301) 843-0159

Sales Tax: CA residents, 7%; DC, 6%. For shipping and handling add \$4.75 for 1-4 books (call for rates for higher quantities). Orders under \$50.00 must be prepaid. Foreign orders must be prepaid. Please allow 4 weeks for delivery. Prices are subject to change without notice. Returns will be accepted within 15 days.

1985 566 pp., illus. Hardback

ISBN 0-915928-94-9

AIAA Members \$54.95

Nonmembers \$81.95

Order Number V-96